

# Deep Active Learning for Solvability Prediction in Power Systems

Yichen Zhang, *Member, IEEE*, Jianzhe Liu, *Member, IEEE*, Feng Qiu, *Senior Member, IEEE*,  
Tianqi Hong, *Member, IEEE*, Rui Yao, *Member, IEEE*

**Abstract**—Traditional methods for solvability region analysis can only have inner approximations with inconclusive conservatism. Machine learning methods have been proposed to approach the real region. In this letter, we propose a deep active learning framework for power system solvability prediction. Compared with the passive learning methods where the training is performed after all instances are labeled, the active learning selects most informative instances to be label and therefore significantly reduce the size of labeled dataset for training. In the active learning framework, the acquisition functions, which correspond to different sampling strategies, are defined in terms of the on-the-fly posterior probability from the classifier. The IEEE 39-bus system is employed to validate the proposed framework, where a two-dimensional case is illustrated to visualize the effectiveness of the sampling method followed by the full-dimensional numerical experiments.

**Index Terms**—Active learning, deep learning, solvability.

## I. INTRODUCTION

In power system security analysis, it is important to quickly assess if power flow has solution (i.e. solvable) given an operation state, and thus it is desirable to develop efficient solvability classifier. However, due to the high-dimensionality of system operation state space, the solvability problem requires extensive samples from the entire space, resulting in very high volumes of samples. Simultaneously, the labeling process requires solving the AC power flow problem of all samples and demands considerable computation resources.

To tackle this challenge, we employ the active learning framework—a family of machine learning methods which *query* the data instances to be labeled for training by an *oracle* (e.g., a human annotator)—to achieve higher accuracy with much fewer labeled examples than passive learning for solvability prediction. Active learning integrates intelligent sampling and machine learning as a closed loop, and it is valuable in problems where unlabeled data are available but obtaining training labels is expensive.

Although sampling towards more informative subspaces has been studied in [1], closed-loop integration of machine learning and intelligent sampling like active learning has not been explored yet. This is the first paper to use deep active learning for solvability prediction to the authors' best knowledge.

This work was supported by the U.S. Department of Energy Office of Electricity – Advanced Grid Modeling Program.

Y. Zhang, J. Liu, F. Qiu, T. Hong and R. Yao are with Argonne National Laboratory, Lemont, IL 60439 USA. Email:yichen.zhang@anl.gov).

## II. DEEP LEARNING FOR POWER FLOW SOLVABILITY APPROXIMATION

Consider an  $N_B$ -bus power network with  $N_G$  generator buses and  $N_D$  load buses. Let  $\mathcal{N}_B$ ,  $\mathcal{N}_G$  and  $\mathcal{N}_D$  denote the set of all buses, generator buses and load buses, respectively.  $\mathcal{N}_{PQ}$  and  $\mathcal{N}_{PV}$  represent sets of PQ and PV buses, respectively. The AC power flow equations are as follows

$$\begin{aligned} P_i^G - P_i^D &= \sum_{j \in \mathcal{N}_B} V_i V_j (G_{ij} \cos \theta_{ij} + B_{ij} \sin \theta_{ij}), i \in \mathcal{N}_{PQ} \cup \mathcal{N}_{PV} \\ Q_i^G - Q_i^D &= \sum_{j \in \mathcal{N}_B} V_i V_j (G_{ij} \sin \theta_{ij} - B_{ij} \cos \theta_{ij}), i \in \mathcal{N}_{PQ} \end{aligned} \quad (1)$$

The bus voltages  $V_i$  and angles  $\theta_i$  are system state variables, and  $\theta_{ij} = \theta_i - \theta_j$ . The existence of solutions to Eq. (1) depends on the values of power injections. To this end, the goal is to build a classifier using a multi-layer perception (MLP) model that can separate the solvable power injections from the non-solvable ones. Therefore, the inputs to the deep neural network are power injections defined as follows

$$\mathbf{X} = [ \mathbf{P}_1^G, \dots, \mathbf{P}_{N_G}^G, \mathbf{Q}_1^G, \dots, \mathbf{Q}_{N_G}^G, \mathbf{P}_1^D, \dots, \mathbf{P}_{N_D}^D, \mathbf{Q}_1^D, \dots, \mathbf{Q}_{N_D}^D ]$$

where  $\mathbf{P}_g^G$  and  $\mathbf{Q}_g^G$  are samples of generation active and reactive power injections at generator bus  $g$ ;  $\mathbf{P}_d^D$  and  $\mathbf{Q}_d^D$  are samples of load active and reactive power injections at load bus  $d$ . Let  $s$ ,  $N_S$  and  $\mathcal{N}_S$  denote sample index, sample numbers and the set of sample indices, respectively. Each sample in  $\mathbf{X}$ , denoted as  $\mathbf{x}_s = \mathbf{X}_{[s,:]}^1$ , will be solved by PSS/E and label its solvability: 0 indicates  $\mathbf{X}_{[s,:]}$  is not solvable and 1 otherwise. To ensure that the generator reactive power samples remain the same in the final solution, we set the reactive power upper and lower limits of all generators to be equal to corresponding samples. We denote the classes of non-solvable and solvable as  $C_q$  for  $q = 1, 2$ , respectively. The label data after one-hot encoding reads

$$\mathbf{Y}^* = \begin{bmatrix} \mathbf{y}_1^* \\ \vdots \\ \mathbf{y}_{N_S}^* \end{bmatrix}, \mathbf{y}_s^* = [ y_{s,1}^*, y_{s,2}^* ] \quad (2)$$

where  $y_{s,q}^* = 1$  indicates that sample  $s$  belongs to class  $q$ . We then apply probabilistic smoothing approximations to the discrete label values. It is well known that when the targets are one-hot encoded and an appropriate loss function is used,

<sup>1</sup>The subscript  $[s, :]$  denotes the sth row of a matrix.

an MLP directly estimates the posterior probability of class membership  $C_q$  conditioned on the input variables  $\mathbf{x}_s$ , denoted by  $p(C_q|\mathbf{x}_s)$ . Denote the MLP classifier as  $\mathbf{y}_s = f(\mathbf{x}_s; \theta)$  where  $\mathbf{y}_s = [y_{s,1}, y_{s,2}] = [p_\theta(C_1|\mathbf{x}_s), p_\theta(C_2|\mathbf{x}_s)]$ , where  $p_\theta(C_q|\mathbf{x})$  for  $q = 1, 2$  denotes the posterior probability of class membership  $q$  given by the classifier under parameter  $\theta$ . The network parameters  $\theta$  can be calculated using the maximum likelihood estimation. Therefore, we minimize the negative logarithm of the likelihood function, known as the cross-entropy loss, as follows

$$L = -\frac{1}{N_s} \sum_{s=1}^{N_s} \sum_{q=1}^2 y_{s,q}^* \log y_{s,q} \quad (3)$$

Since the output values of the MLP are interpreted as probabilities, they each must lie in the range (0,1), and they must sum to unity. This can be achieved by using a *softmax* activation function at the output layer of the MLP.

### III. ACTIVE LEARNING FRAMEWORK

Assume we randomly generate a feature set  $\mathcal{X}$  that is sufficiently large to represent the underlying physical features. In traditional *passive* supervised learning methods, we will generate labels for the entire feature set  $\mathcal{X}$ , denoted as  $\mathcal{Y}_{\mathcal{X}}$ , using the simulation software and result parser, which is regarded as the oracle. The labeling process is computationally demanding if the data set is large and becomes intractable for high-dimensional problems. This is known as the *labeling bottleneck*, which occurs not only in power systems but also in computer vision, natural language processing, and other machine learning tasks. The active learning framework can overcome such a labeling bottleneck. The batch-mode active learning algorithm's pseudocode is presented in Algorithm 1. Obviously, the querying strategy  $a(\cdot, \cdot)$  differentiates the active learning from passive learning algorithms. In other words, active learning under the random querying strategy will be equivalent to passive learning algorithms. The queries can be either selected in serial (one at a time) or batches (several to be labeled at once). Algorithm 1 is the batch-mode active learning. Given the machine learning model  $f$ , unlabeled pool  $\mathcal{U}$ , and inputs  $\mathbf{X} \in \mathcal{U}$ , the querying strategy can be represented as a function  $a$ , which is referred to as the *acquisition function* written as follows

$$\mathbf{x}^* = \arg \max_{\mathbf{x} \in \mathcal{U}} a(\mathbf{X}, f(\cdot; \theta)) \quad (4)$$

where  $\mathbf{x}^*$  denotes the most informative sample selected by the corresponding strategy.

#### A. Query Strategy: Uncertainty Sampling

The query strategy aims at evaluating the informativeness of unlabeled instances. There have been many proposed ways of formulating such query strategies in the literature. Interested readers can refer to [2] for more details. Among all frameworks, the most widely used and computationally efficient methodology is uncertainty sampling. In this letter, an active learner queries the most difficult instances to classify by the

deep learning model trained at the current stage. When interpreting the binary classification using a probabilistic model, uncertainty sampling queries the instance whose posterior probability provided by the classifier is the closest to 0.5 [2]. In other words, the selected sample is the least confident to the classifier. For a general multi-class problem, this *least confident sampling* [2] can be expressed as follows

$$\mathbf{x}_{\text{LC}}^* = \operatorname{argmin}_{\mathbf{x} \in \mathcal{U}} \max_{q=1,2} p_\theta(C_q|\mathbf{x}) \quad (5)$$

In the case of multi-class classification, this metric omits information about the remaining labels. To compensate this omission, the *margin sampling* is introduced as follows

$$\mathbf{x}_{\text{M}}^* = \operatorname{argmin}_{\mathbf{x} \in \mathcal{U}} |p_\theta(C_2|\mathbf{x}) - p_\theta(C_1|\mathbf{x})| \quad (6)$$

Besides the aforementioned metrics, the *entropy sampling* is also widely used to measure the amount of information that is encoded and can be only as a metric in active learning

$$\mathbf{x}_{\text{E}}^* = \operatorname{argmax}_x \left( -\sum_{q=1}^2 p_\theta(C_q|\mathbf{x}) \log p_\theta(C_q|\mathbf{x}) \right) \quad (7)$$

As pointed out in [2] and many other references, although all strategies generally outperform passive baselines, the best strategy may be application-dependent. Thus, we apply all three strategies to the solvability problem in this letter.

### IV. CASE STUDY

We use the IEEE 39-bus system and the PSS/E software to demonstrate the framework. The deep neural net is shown in Fig. (1). First, we illustrate a two-dimensional case for visualization purposes. In this case, we uniformly sample active power loads at Buses 3 and 4 from  $-3000$  MW to  $3000$  MW. Before the training starts, all samples are normalized. We allocate 80% samples for training and 20% samples for testing. The active learner randomly selects 100 samples from the training dataset to label for the initial training phase and queries ten instances in each iteration using the margin sampling strategy. The algorithm terminates if the averaged testing accuracy of the last four iterations is greater than 99% or the algorithm reaches 30 iterations. The margin sampling strategy terminates after seven iterations, and achieves 99.1% accuracy with only 170 labeled samples. While the random strategy fails to meet the accuracy criterion after 30 iterations, achieving only 98.9% accuracy with 400 labeled samples. Samples that are queried by the active learner are plotted in Fig. 2, where the decision boundary of the neural network is illustrated using the colored areas (the blue area is solvable). Meanwhile, labeled dataset in the background indicates the estimation is not conservatism. As one can observe, the margin sampling strategy precisely selects instances at the solvability boundary, indicating significantly high sampling efficiency.

Second, a high-dimensional scenario is illustrated. Except for the slack bus (Generator 39 at Bus 10), active and reactive power outputs of all generators are sampled uniformly between the dispatchable limits. Meanwhile, active and reactive power demands of all loads are sampled using normal distributions, which use the base values as the means and admit 50%

---

**Algorithm 1:** Batch-mode active learning algorithm
 

---

**input :** Labeled set  $\mathcal{L}$ , unlabeled set  $\mathcal{U}$ , query strategy  $a(\cdot, \cdot)$ , query batch size  $B$ , labeling oracle  $\text{Oracle}(\cdot)$ , deep neural net  $f(\cdot; \theta)$ , neural network training function  $\text{Train}(\cdot, \cdot)$

$\mathcal{A} \leftarrow \emptyset$  // initialize the set to store acquisition instances

**repeat**

$\theta \leftarrow \text{Train}(\mathcal{L}, f(\cdot; \theta))$  // train the model using current  $\mathcal{L}$

**for**  $i \leftarrow 1$  **to**  $B$  **do**

$\mathbf{x}_i^* \leftarrow \arg \max_{\mathcal{U}} a(\mathcal{U}, f(\cdot; \theta))$  // query the instance from the unlabeled set

$\mathbf{y}_i^* \leftarrow \text{Oracle}(\mathbf{x}_i^*)$  // label the acquisition instance

$\mathcal{L} \leftarrow \mathcal{L} \cup \langle \mathbf{x}_i^*, \mathbf{y}_i^* \rangle$  // add the labeled query to  $\mathcal{L}$

$\mathcal{U} \leftarrow \mathcal{U} - \mathbf{x}_i^*$  // remove the labeled query from  $\mathcal{U}$

$\mathcal{A} \leftarrow \mathcal{A} \cup \langle \mathbf{x}_i^*, \mathbf{y}_i^* \rangle$  // store the acquisition instance

**end**

**until** some stopping criterion;

**output:** Trained deep neural net  $f(\cdot; \theta)$ , all acquisition instances  $\mathcal{A}$

---

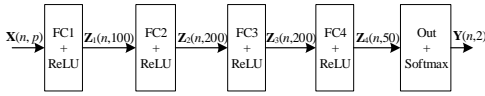


Fig. 1. The structure of the deep neural network.

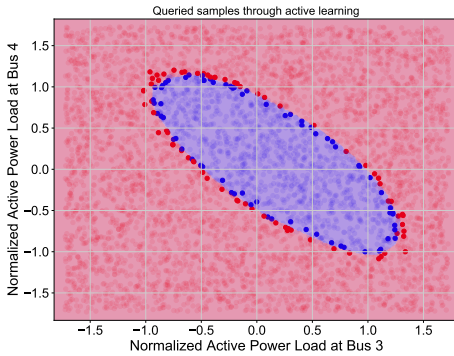


Fig. 2. Queried instances by the margin sampling strategy, which precisely selects instances at the solvability boundary. The blue area denotes the solvability region predicted by the neural network. Labeled dataset in the background indicates the estimation is not conservatism.

standard deviation. In total, we have 57 features. All samples are normalized, among which 80% samples are allocated for training and 20% samples for testing. In the active learning, 10000 samples are randomly selected for the initial training phase followed by 6000-sample query iterations. We perform ten iterations and compare all the aforementioned sample strategies, including random (baseline), least-confident, margin, and entropy. We conduct five runs with different random seeds and illustrate the results in Fig. 3. We expect that the least-confident and margin to have equal performance since Eqs. (5) and (6) are equivalent under binary classification problems. The results also show that the least-confident and margin methods outperform entropy sampling. All three active learning methods are superior to the random sampling. Compared with the random strategy, margin and least-confident achieve mostly 10% accuracy improvement while the entropy-

based method admits 5% improvement. The margin and least-confident methods also have fewer performance variations compared to the entropy-based method. To achieve the same accuracy of margin and least-confident methods, the random baseline will need 36000 samples, which is five times more.

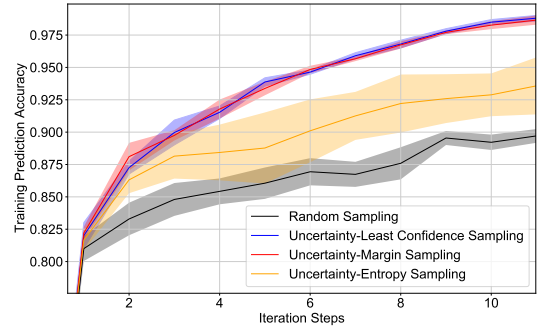


Fig. 3. Training accuracy of different sampling strategies. The solid lines indicate the mean values while the shaded areas represent the standard deviations.

## V. CONCLUSIONS

This letter proposes the deep active learning method for power system solvability prediction. The active sampling strategies can select the most informative instances to be labeled and facilitate the predictor accuracy with fewer samples and labeling efforts. The sampling effectiveness is illustrated in a two-dimensional case. Four different sampling strategies are then compared in the high-dimensional solvability prediction. The results indicate that the active learning significantly outperforms passive methods.

## REFERENCES

- [1] V. Krishnan and J. D. McCalley, "Importance sampling based intelligent test set generation for validating operating rules used in power system operational planning," *IEEE Trans. Power Syst.*, vol. 28, no. 3, pp. 2222–2231, 2013.
- [2] B. Settles, "Active learning literature survey," University of Wisconsin-Madison Department of Computer Sciences, Tech. Rep., 2009.